Acta Mech 232, 2513–2533 (2021)
https://doi.org/10.1007/s00707-021-02955-0

ORIGINAL PAPER

Keqiang Hu · S. A. Meguid · Libin Wang · Hui Jin

Electro-elastic field of a piezoelectric quasicrystal medium containing two cylindrical inclusions

Received: 23 December 2020 / Revised: 27 January 2021 / Accepted: 1 February 2021 / Published online: 15 April 2021

Abstract Considering the piezoelectric effect, the electro-elastic field of an infinite one-dimensional quasicrystal medium with two circular cylindrical inclusions is derived under antiplane shear and inplane electric loading. The boundary value problem of the composite material with circular cylindrical inclusions is analytically solved by the use of the conformal mapping technique and analytical continuation theory. The stresses in the phonon and phason fields and the electric displacements are obtained explicitly in the form of a power series both for the matrix and the inclusions. Some typical examples are analyzed to show the effect of the geometric parameters, material properties, and electro-mechanical loading on the electro-elastic fields in the matrix, inclusions, and interfaces. The limiting cases of circular cavities and rigid circular inclusions have also been investigated and discussed.

1 Introduction

As a new class of condensed matters with quasi-periodic translational symmetry and non-crystallographic rotational symmetry, quasicrystals (QCs) have been reported by Shechtman et al. [1]. QCs differ from the conventional crystalline materials and non-crystalline materials and possess long-range order and no translational periodicity, and due to their ordered patterns, many unusual and remarkable properties have been in QCs, such as low friction coefficient, high hardness, low thermal conductivity, which make them highly desirable for extensive engineering applications [2, 3].

Note that a one-dimensional quasicrystal (1D QC) is defined as a three-dimensional solid whose atomic structures are periodic in the $(x_1 - x_2)$-plane and quasiperiodic in the normal direction of the plane. Thus, there only exists a phason displacement w_3 along the x_3- axis for describing the quasilattices, and 1D QCs show a property of transverse isotropy [4]. QCs may contain multiple defects such as inclusions, holes, and cracks. When QCs are subjected to external loadings, these defects coalesce and grow leading to damage and/or failure of this class of materials. Therefore, it is meaningful to study the problems of quasicrystal materials (QCs)

K. Hu (✉)
State Key Laboratory of Mechanics and Control of Mechanical Structures, Nanjing University of Aeronautics and Astronautics, Nanjing 210016, China
e-mail: keqianghu@163.com

S. A. Meguid (✉)
Department of Mechanical and Industrial Engineering, University of Toronto, 5 King's Road, Toronto M5S 3G8, Canada
e-mail: meguid@mie.utoronto.ca

L. Wang
School of Civil Engineering, Nanjing Forestry University, Nanjing 210037, Jiangsu, China

H. Jin
Department of Engineering Mechanics, Southeast University, Nanjing 210096, China

containing cracks or inclusions. Fan et al. [5] studied the problem of a moving screw dislocation in a one-dimensional hexagonal quasicrystal and obtained analytical solutions for the stress field. Collinear periodic cracks and/or rigid line inclusions of antiplane sliding mode in a one-dimensional hexagonal quasicrystal have been investigated by Shi [6]. The two-dimensional problem of an elliptic hole or a crack in three-dimensional quasicrystals subject to far-field loadings was analyzed based on the complex potential method [7]. A path-independent integral in fracture mechanics of quasicrystals has been derived to evaluate the fracture parameters in QCs with the atomic arrangement being quasi-periodic in one, two or three directions. Furthermore, the relation between the stress intensity factor and energy release rate was discussed by Sladek et al. [8]. Loboda et al. [9] presented an analytical approach of an electrically permeable interface crack in a 1D piezoelectric quasicrystal. The interaction of a screw dislocation and an elliptical hole with 2 asymmetric cracks in a one-dimensional hexagonal piezoelectric quasicrystal has been considered, and the general solutions of the elastic and electric fields have been derived in Li et al. [10].

Piezoelectric quasicrystal materials are expected to be exploited as sensors and actuators in smart structures [11]. Li et al. [12] obtained three-dimensional fundamental solutions for a one-dimensional hexagonal quasicrystal with piezoelectric effect, and the solutions are explicitly expressed in terms of elementary functions. Within a framework of the state space method, an axisymmetric solution for a functionally graded one-dimensional hexagonal piezoelectric quasicrystal circular plate has been presented by Li et al. [13]. Using the complex variable formulations and the conformal mapping technique, Yang and Li [14] investigated the antiplane shear problem of two symmetric cracks originating from an elliptical hole in 1D hexagonal piezoelectric QC. General solutions of plane problems in 1D piezoelectric QC material have been obtained based on the fundamental equations of piezoelectricity. Furthermore, the application of fracture mechanics of QCs was discussed by Yu et al. [15]. Fan et al. [16] obtained the fundamental solution of three-dimensional cracks in one-dimensional hexagonal piezoelectric quasicrystals. The problem of an antiplane crack in a half-space of a one-dimensional piezoelectric quasicrystal is studied by Tupholme [17] using an extension of the classical continuous dislocation layer method. Li et al. [18] performed the fracture analysis of a transversely isotropic piezoelectric quasicrystal cylinder under axial shear and found that the quasicrystal fracture is governed by the phonon or phason field, depending on the phonon-phason loading ratio. A moving crack in 1D hexagonal piezoelectric quasicrystals was considered under antiplane shear and inplane electric field, and the result shows that the coupled elastic fields inside piezoelectric QCs depend on the speed of crack propagation [19]. An interface crack between dissimilar 1D hexagonal QCs with piezoelectric effect under antiplane shear loading and inplane electric field has been studied by Hu et al. [20] using singular integral equation method. The extended displacement discontinuity boundary integral–differential equation method has been applied to analyze a three-dimensional arbitrarily shaped interface crack in a one-dimensional hexagonal thermo-electro-elastic QC bi-material [21, 22].

When the inclusions are embedded in an elastic medium, the differences between the material properties of matrix and inclusions may disturb the stress fields around and inside the inclusions, as shown by Honein et al. [23] and Wu [24]. Based on the method of complex stress potentials, Zou and Li [25] investigated the stresses around two similar circular cylindrical inclusions in an infinite medium under the generalized plane strain conditions. Ma and Gao [26] provided the fourth-order Eshelby tensor for a plane strain inclusion of arbitrary cross-sectional shape in a general form, and the numerical results show that the derived Eshelby tensor depends on both the position and inclusion size.

Considering the piezoelectric effect, Deeg [27] examined the effect of a dislocation, a crack, and an inclusion upon the coupled response of a piezoelectric medium. A theoretical treatment was provided for the elliptical inhomogeneity problem in piezoelectric materials under antiplane shear and inplane electric field using the complex variable method [28]. Wu and Kunio [29] derived the electro-elastic field of an infinite piezoelectric medium with two circular cylindrical inclusions, and the analytical solutions have been obtained. The interactions between **N** randomly distributed cylindrical inclusions in a piezoelectric matrix have been studied by Yang et al. [30], and it was shown that the electro-elastic field distribution in a piezoelectric material with multiple inclusions is significantly different from that in the case of a single inclusion. He and Lim [31] studied the electro-mechanical response of piezoelectric fibrous composites with viscous interface under antiplane shear stress state, and the obtained result was used to study the overall behavior of the composite based on the Mori–Tanaka mean field approximation scheme. The interaction between a screw dislocation and a piezoelectric circular inclusion with viscous interface has been studied by Wang et al. [32], and exact closed-form solutions in terms of elementary functions were derived for the time-dependent electro-elastic fields. Using the method of harmonic functions, a closed-form solution for a spherical inclusion in an infinite

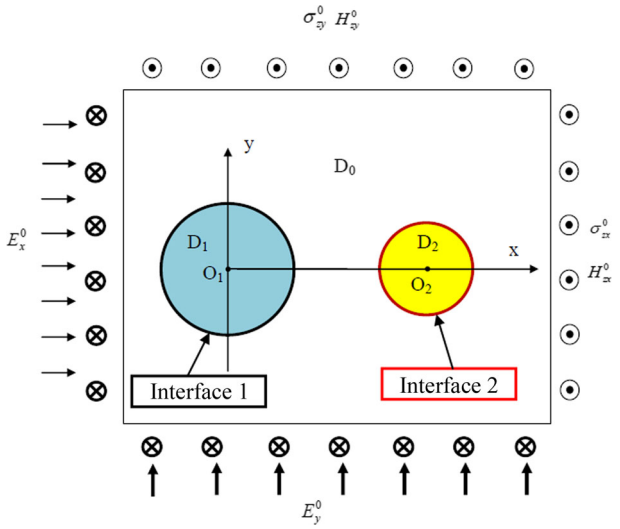

Fig. 1 Two circular cylindrical inclusions under antiplane shear and inplane electric loading

1D hexagonal quasicrystal matrix with piezoelectric effect under general homogeneous loading was obtained by Zhang et al. [33].

To the authors' knowledge, the problem of 2 circular cylindrical inclusions in an infinite 1D piezoelectric QC under antiplane shear and inplane electric loading has not been reported. In this work, the interaction between two circular cylindrical inclusions in an infinite 1D QC medium is studied by the complex variable method. The boundary value problem is analytically solved by applying the conformal mapping technique and the analytical continuation theory. Exact solutions of the phonon field stresses, phason field stresses and electric displacements in the inclusions and matrix are obtained. Finally, some typical examples are analyzed to show the effect of the geometric parameters, material properties and electro-mechanical loading on the electro-elastic fields in the matrix, inclusions, and interfaces.

2 Problem statement

We consider an infinite one-dimensional (1D) piezoelectric quasicrystal (QC) matrix containing 2 1D piezoelectric quasicrystal circular cylindrical inclusions which are parallel to each other and infinitely long along the direction perpendicular to the xy-plane, as shown in Figs. 1 and 2. Both the matrix and inclusions are assumed to be transversely isotropic with a quasi-periodic poling axis along the z-axis, which is vertical to the xy-plane. The regions occupied by the matrix, inclusion-1 and inclusion-2 are referred to as regions 0, 1, and 2, respectively. The two circular cylindrical inclusions have radii r_1 and r_2, respectively, and the distance between the two axes of the two inclusions is h, and $h > r_1 + r_2$. The interfaces between the matrix and the two circular inclusions are denoted by interface 1 and interface 2, respectively.

As shown in Fig. 1, the infinite one-dimensional (1D) piezoelectric quasicrystal (QC) matrix is subjected to uniform inplane electric fields E_x^0 and E_y^0, and uniform antiplane shear in the phonon and phason fields, σ_{zy}^0, σ_{zx}^0 and H_{zy}^0, H_{zx}^0, at infinity, respectively. The material constants of the two circular cylindrical inclusions are general and unconstrained. The interfaces between the circular cylindrical inclusions and matrix are assumed to be perfectly bonded.

For the current boundary value problem, the deformation is independent of the spatial variable z, i.e., only the non-vanishing antiplane displacements of phonon and phason fields and inplane electric fields are considered:

$$u_z = u_z(x, y),\ w_z = w_z(x, y),\ \varphi = \varphi(x, y) \tag{1}$$

where u_z and w_z are components of the displacement vector of phonon and phason fields, respectively, and φ is the electric potential.

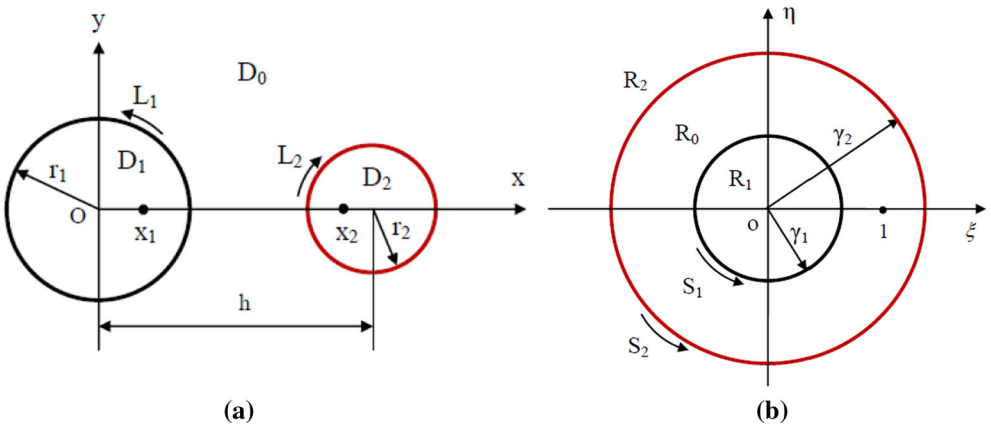

Fig. 2 Conformal transformation

According to the quasicrystal elasticity theory and considering the piezoelectric effect, the constitutive relations for the present antiplane problem are [20]

$$\begin{Bmatrix} \sigma_{zx} \\ H_{zx} \\ D_x \end{Bmatrix} = \begin{bmatrix} c_{44} & R_3 & e_{15} \\ R_3 & K_2 & d_{15} \\ e_{15} & d_{15} & -\lambda_{11} \end{bmatrix} \begin{Bmatrix} \varepsilon_{zx} \\ \gamma_{zx} \\ -E_x \end{Bmatrix}, \begin{Bmatrix} \sigma_{zy} \\ H_{zy} \\ D_y \end{Bmatrix} = \begin{bmatrix} c_{44} & R_3 & e_{15} \\ R_3 & K_2 & d_{15} \\ e_{15} & d_{15} & -\lambda_{11} \end{bmatrix} \begin{Bmatrix} \varepsilon_{zy} \\ \gamma_{zy} \\ -E_y \end{Bmatrix} \tag{2}$$

where c_{44} K_2 and R_3 are the respective phonon field elastic constant, the phason field elastic constant, and the phonon-phason coupling constant; e_{15} and d_{15} are the respective piezoelectric coefficients, and λ_{11} is the dielectric permittivity. Additionally, σ_{zj}, H_{zj} and ε_{zj}, γ_{zj} $(j = x, y)$ are the respective stresses and strains in the phonon and the phason fields, and D_j and E_j $(j = x, y)$ are the electric displacement and electric field, respectively.

The gradient equations are as follows:

$$\varepsilon_{zj} = u_{z,j},\ \gamma_{zj} = w_{z,j},\ E_j = -\varphi_{,j} \quad j = x, y \tag{3}$$

where a comma implies partial differentiation with respect to the coordinate.

The equilibrium equations of the 1D piezoelectric QC under antiplane deformation and inplane electric loading are:

$$\sigma_{zj,j} = 0,\ H_{zj,j} = 0,\ D_{j,j} = 0. \tag{4}$$

By considering the constitutive relations and the gradient equations and neglecting body forces and free charge, the governing equations for the antiplane problem of the 1D piezoelectric QC can be obtained as

$$\begin{bmatrix} c_{44} & R_3 & e_{15} \\ R_3 & K_2 & d_{15} \\ e_{15} & d_{15} & -\lambda_{11} \end{bmatrix} \begin{Bmatrix} \nabla^2 u_z \\ \nabla^2 \varphi \\ \nabla^2 w_z \end{Bmatrix} = \begin{Bmatrix} 0 \\ 0 \\ 0 \end{Bmatrix} \tag{5}$$

where $\nabla^2 = \partial^2/\partial x^2 + \partial^2/\partial y^2$ is the two-dimensional Laplacian operator in the variables x and y. From Eq. (5), it can be seen that u_z, φ, and w_z satisfy the Laplacian equation when the determinant $\begin{vmatrix} c_{44} & R_3 & e_{15} \\ R_3 & K_2 & d_{15} \\ e_{15} & d_{15} & -\lambda_{11} \end{vmatrix} \neq 0$, which is the most general case. The solution of u_z φ and w_z can then be expressed as the real parts of the analytic functions $U(z)$, $\Phi(z)$ and $W(z)$ as:

$$u_z = \mathrm{Re}[U(z)]/c_{44},\ \varphi = \mathrm{Re}[\Phi(z)]/\lambda_{11},\ w_z = \mathrm{Re}[W(z)]/K_2 \tag{6}$$

where $z = x + iy$ $(i = \sqrt{-1})$ is the complex variable and the over-bar refers to the complex conjugate. "Re" denotes the real part of a complex number.

The strains, stresses in the phonon field, the electric fields, electric displacements and the strains and stresses in the phason field can be expressed in terms of the complex field potentials $U(z)$, $\Phi(z)$ and $W(z)$ as

$$\begin{Bmatrix} \varepsilon_{zx} \\ E_x \\ \gamma_{zx} \end{Bmatrix} - i \begin{Bmatrix} \varepsilon_{zy} \\ E_y \\ \gamma_{zy} \end{Bmatrix} = \begin{Bmatrix} U'(z)/c_{44} \\ -\Phi'(z)/\lambda_{11} \\ W'(z)/K_2 \end{Bmatrix}, \tag{7}$$

$$\begin{Bmatrix} \sigma_{zx} \\ D_x \\ H_{zx} \end{Bmatrix} - i \begin{Bmatrix} \sigma_{zy} \\ D_y \\ H_{zy} \end{Bmatrix} = \begin{bmatrix} 1 & e_{15}/\lambda_{11} & R_3/K_2 \\ e_{15}/c_{44} & -1 & d_{15}/K_2 \\ R_3/c_{44} & d_{15}/\lambda_{11} & 1 \end{bmatrix} \begin{Bmatrix} U'(z) \\ \Phi'(z) \\ W'(z) \end{Bmatrix} \tag{8}$$

where the primed quantities denote the derivatives with respect to the arguments.

The resultant force in the phonon field T, the resultant normal component N of the electric displacement and the resultant force in the phason field M along any arc ac can be expressed as

$$\begin{Bmatrix} T \\ N \\ M \end{Bmatrix} = \int_a^c \left(\begin{Bmatrix} \sigma_{zx} \\ D_x \\ H_{zx} \end{Bmatrix} dy - \begin{Bmatrix} \sigma_{zy} \\ D_y \\ H_{zy} \end{Bmatrix} dx \right) = \mathrm{Im} \left[\begin{bmatrix} 1 & e_{15}/\lambda_{11} & R_3/K_2 \\ e_{15}/c_{44} & -1 & d_{15}/K_2 \\ R_3/c_{44} & d_{15}/\lambda_{11} & 1 \end{bmatrix} \begin{Bmatrix} U(z) \\ \Phi(z) \\ W(z) \end{Bmatrix} \right]_a^c \tag{9}$$

where $[]_a^c$ represents the change in the bracketed function going from point a to point c along the arc ac, and "Im" denotes the imaginary part of a complex number.

To simplify the analysis, we introduce a new complex variable $\zeta (\zeta = \xi + i\eta)$ by the following bilinear transformation:

$$\begin{aligned} & z = \Omega(\zeta) = \frac{x_2\zeta - x_1}{\zeta - 1}, \ \zeta = \Omega^{-1}(z) = \frac{z - x_1}{z - x_2}, \\ & x_1 x_2 = r_1^2, \ (h - x_1)(h - x_2) = r_2^2, \\ & x_1 = r_1 b, \ x_2 = r_1/b, \\ & b = \frac{h^2 + r_1^2 - r_2^2 - \sqrt{(h^2 + r_1^2 - r_2^2)^2 - 4r_1^2 h^2}}{2r_1 h} \end{aligned} \tag{10}$$

where x_1 and x_2(Fig. 2a) are the points, symmetrical relative to the circumferential L_1 and L_2, respectively, and h is the distance between the two axes of the two circular cylindrical inclusions, with radii of r_1 and r_2, respectively. The positive directions of the boundary contours are indicated by arrows in Figs. 2. The respective circles L_1 and L_2 are transformed into the concentric circles S_1 and S_2 with radii

$$\gamma_1 = \sqrt{\frac{x_1}{x_2}}, \ \gamma_2 = \sqrt{\frac{h - x_1}{h - x_2}}. \tag{11}$$

It is to be noted that the points at infinity in the original plane are transformed into internal points in the ring, $(\xi, \eta) = (1, 0)$, in the transformed plane, as shown in Fig. 2b.

Considering the relations shown in Eq. (10), Eqs. (6–9) can be expressed in the ζ–plane as:

$$u_z(\zeta) = \mathrm{Re}[U(\zeta)]/c_{44}, \ \varphi(\zeta) = \mathrm{Re}[\Phi(\zeta)]/\lambda_{11}, \ w_z(\zeta) = \mathrm{Re}[W(\zeta)]/K_2, \tag{12}$$

$$\varepsilon_{zx} - i\varepsilon_{zy} = \frac{U'(\zeta)}{c_{44}\Omega'(\zeta)}, \ E_x - iE_y = -\frac{\Phi'(\zeta)}{\lambda_{11}\Omega'(\zeta)}, \ \gamma_{zx} - i\gamma_{zy} = \frac{W'(\zeta)}{K_2\Omega'(\zeta)}, \tag{13}$$

$$\begin{Bmatrix} \sigma_{zx} \\ D_x \\ H_{zx} \end{Bmatrix} - i \begin{Bmatrix} \sigma_{zy} \\ D_y \\ H_{zy} \end{Bmatrix} = \frac{1}{\Omega'(\zeta)} \begin{bmatrix} 1 & e_{15}/\lambda_{11} & R_3/K_2 \\ e_{15}/c_{44} & -1 & d_{15}/K_2 \\ R_3/c_{44} & d_{15}/\lambda_{11} & 1 \end{bmatrix} \begin{Bmatrix} U'(\zeta) \\ \Phi'(\zeta) \\ W'(\zeta) \end{Bmatrix}, \tag{14}$$

$$\begin{Bmatrix} T \\ N \\ M \end{Bmatrix} = \mathrm{Im} \left[\begin{bmatrix} 1 & e_{15}/\lambda_{11} & R_3/K_2 \\ e_{15}/c_{44} & -1 & d_{15}/K_2 \\ R_3/c_{44} & d_{15}/\lambda_{11} & 1 \end{bmatrix} \begin{Bmatrix} U(\zeta) \\ \Phi(\zeta) \\ W(\zeta) \end{Bmatrix} \right]_a^c \tag{15}$$

where $U(\zeta)$, $\Phi(\zeta)$, and $W(\zeta)$ represent $U(\Omega(\zeta))$, $\Phi(\Omega(\zeta))$, and $W(\Omega(\zeta))$, respectively.

For a homogeneous one-dimensional piezoelectric quasicrystal medium, when the uniform antiplane shear and inplane electric loadings are applied at infinity, as shown in Fig. 1, the corresponding boundary conditions at infinity can be expressed as

$$\begin{Bmatrix} \sigma_{zx}^0 \\ E_x^0 \\ H_{zx}^0 \end{Bmatrix} - i \begin{Bmatrix} \sigma_{zy}^0 \\ E_y^0 \\ H_{zy}^0 \end{Bmatrix} = \lim_{z\to\infty} \begin{bmatrix} 1 & \alpha_{10} & \alpha_{20} \\ 0 & -1/\lambda_{11}^0 & 0 \\ \delta_{10} & \delta_{20} & 1 \end{bmatrix} \begin{Bmatrix} U'(z) \\ \Phi'(z) \\ W'(z) \end{Bmatrix} \tag{16}$$

where the constants α_{10}, α_{20}, δ_{10}, δ_{20} are defined as

$$\begin{aligned} &\alpha_{10} = e_{15}^0/\lambda_{11}^0,\ \alpha_{20} = R_3^0/K_2^0, \\ &\delta_{10} = R_3^0/c_{44}^0,\ \delta_{20} = d_{15}^0/\lambda_{11}^0. \end{aligned} \tag{17}$$

The assumption of the perfect bonding interface between the two circular cylindrical inclusions and matrix leads to the continuity of the displacements, electric potential, resultant forces, and resultant normal component of electric displacement across the interfaces, i.e.,

$$\frac{u_z^0 = u_z^j,\ w_z^0 = w_z^j,\ \varphi_0 = \varphi_j}{T_0 = T_j,\ P_0 = P_j,\ M_0 = M_j} \quad (j = 1, 2) \tag{18}$$

where the superscript or subscript $j = 1$ or 2 denotes the quantities referring to the region D_1, R_1 or D_2, R_2, which corresponds to the inclusion 1 or 2; the superscript or subscript $j = 0$ denotes the quantities referring to the region D_0, R_0 of the matrix.

Accordingly, the interface boundary conditions in the transformed plane on $|\zeta| = \gamma_j$ can be expressed as

$$\begin{aligned} &\mathrm{Re}[U_0(\zeta)] = \beta_{1j}\mathrm{Re}\big[U_j(\zeta)\big] \\ &\mathrm{Re}[\Phi_0(\zeta)] = \beta_{2j}\mathrm{Re}\big[\Phi_j(\zeta)\big] \quad (j = 1, 2), \\ &\mathrm{Re}[W_0(\zeta)] = \beta_{3j}\mathrm{Re}\big[W_j(\zeta)\big] \end{aligned} \tag{19}$$

$$\begin{bmatrix} 1 & \alpha_{10} & \alpha_{20} \\ \mu_{10} & -1 & \mu_{20} \\ \delta_{10} & \delta_{20} & 1 \end{bmatrix} \begin{Bmatrix} \mathrm{Im}[U_0(\zeta)] \\ \mathrm{Im}[\Phi_0(\zeta)] \\ \mathrm{Im}[W_0(\zeta)] \end{Bmatrix} = \begin{bmatrix} 1 & \alpha_{1j} & \alpha_{2j} \\ \mu_{1j} & -1 & \mu_{2j} \\ \delta_{1j} & \delta_{2j} & 1 \end{bmatrix} \begin{Bmatrix} \mathrm{Im}\big[U_j(\zeta)\big] \\ \mathrm{Im}\big[\Phi_j(\zeta)\big] \\ \mathrm{Im}\big[W_j(\zeta)\big] \end{Bmatrix} \quad (j = 1, 2) \tag{20}$$

where the constants β_{1j}, β_{2j}, β_{3j} $(j = 1, 2)$ and α_{1j}, α_{2j}, δ_{1j}, δ_{2j}, μ_{1j}, μ_{2j} $(j = 0, 1, 2)$ are defined as

$$\beta_{1j} = c_{44}^0\Big/c_{44}^j,\ \beta_{2j} = \lambda_{11}^0\Big/\lambda_{11}^j,\ \beta_{3j} = K_2^0\Big/K_2^j \quad (j = 1, 2), \tag{21}$$

$$\begin{aligned} &\alpha_{1j} = e_{15}^j\Big/\lambda_{11}^j,\ \alpha_{2j} = R_3^j\Big/K_2^j, \\ &\delta_{1j} = R_3^j\Big/c_{44}^j,\ \delta_{2j} = d_{15}^j\Big/\lambda_{11}^j \quad j = 0, 1, 2, \\ &\mu_{1j} = e_{15}^j\Big/c_{44}^j,\ \mu_{2j} = d_{15}^j\Big/K_2^j. \end{aligned} \tag{22}$$

Considering the fact that the infinity point in the original plane corresponds to the point $(1, 0)$ in the transformed plane, as shown in Fig. 2, the corresponding boundary conditions at infinity in the transformed plane can be expressed as

$$\begin{Bmatrix} \sigma_{zx}^0 - i\sigma_{zy}^0 \\ E_x^0 - iE_y^0 \\ H_{zx}^0 - iH_{zy}^0 \end{Bmatrix} = \lim_{\zeta\to 1} \left(\frac{(\zeta-1)^2}{x_1 - x_2} \begin{bmatrix} 1 & \alpha_{10} & \alpha_{20} \\ 0 & -1/\lambda_{11}^0 & 0 \\ \delta_{10} & \delta_{20} & 1 \end{bmatrix} \begin{Bmatrix} U_0'(\zeta) \\ \Phi_0'(\zeta) \\ W_0'(\zeta) \end{Bmatrix} \right). \tag{23}$$

3 Solution to the boundary value problem

In this Section, the theorem of analytic continuation is applied to solve the present boundary value problem. It can be observed from Eq. (23) that $U_0(\zeta)$, $\Phi_0(\zeta)$, and $W_0(\zeta)$ have the pole (singular point) of order one at point $\zeta = 1$. Thus, it can be set as follows:

$$\begin{Bmatrix} U_0(\zeta) \\ \Phi_0(\zeta) \\ W_0(\zeta) \end{Bmatrix} = \frac{1}{\zeta - 1} \begin{Bmatrix} u_0(\zeta) \\ \phi_0(\zeta) \\ w_0(\zeta) \end{Bmatrix} \tag{24}$$

where $u_0^{'}(1)$, $\phi_0^{'}(1)$, $w_0^{'}(1)$ are finite and the following results can be derived from Eq. (23) as

$$\begin{Bmatrix} u_0(1) \\ \phi_0(1) \\ w_0(1) \end{Bmatrix} = (x_2 - x_1) \begin{bmatrix} 1 & \alpha_{10} & \alpha_{20} \\ 0 & -1/\lambda_{11}^0 & 0 \\ \delta_{10} & \delta_{20} & 1 \end{bmatrix}^{-1} \begin{Bmatrix} \sigma_{zx}^0 - i\sigma_{zy}^0 \\ E_x^0 - iE_y^0 \\ H_{zx}^0 - iH_{zy}^0 \end{Bmatrix}. \tag{25}$$

Considering that the functions $U_0(\zeta)$, $\Phi_0(\zeta)$, $W_0(\zeta)$ are analytic in region R_0, the functions $u_0(\zeta)$, $\phi_0(\zeta)$, $w_0(\zeta)$ also are analytic in R_0. After some manipulation of Eqs. (19), (20), and (24), we can obtain the following relations:

$$\begin{Bmatrix} u_0(\zeta) \\ \phi_0(\zeta) \\ w_0(\zeta) \end{Bmatrix} = \frac{\zeta - 1}{2} \left(\left[\left[B_j \right] + \left[B_{0j} \right] \right] \begin{Bmatrix} U_j(\zeta) \\ \Phi_j(\zeta) \\ W_j(\zeta) \end{Bmatrix} + \left[\left[B_j \right] - \left[B_{0j} \right] \right] \begin{Bmatrix} \overline{U_j(\zeta)} \\ \overline{\Phi_j(\zeta)} \\ \overline{W_j(\zeta)} \end{Bmatrix} \right) \quad (|\zeta| = \gamma_j) \tag{26}$$

where the matrices $\left[\mathbf{B}_{0j}\right]$ and $\left[\mathbf{B}_j\right]$ $(j = 1, 2)$ are defined as

$$\begin{aligned} \left[B_{0j} \right] &= \begin{bmatrix} 1 & \alpha_{10} & \alpha_{20} \\ \mu_{10} & -1 & \mu_{20} \\ \delta_{10} & \delta_{20} & 1 \end{bmatrix}^{-1} \begin{bmatrix} 1 & \alpha_{1j} & \alpha_{2j} \\ \mu_{1j} & -1 & \mu_{2j} \\ \delta_{1j} & \delta_{2j} & 1 \end{bmatrix} \quad (j = 1, 2), \\ \left[B_j \right] &= \begin{bmatrix} \beta_{1j} & 0 & 0 \\ 0 & \beta_{2j} & 0 \\ 0 & 0 & \beta_{3j} \end{bmatrix}. \end{aligned} \tag{27}$$

According to the Laurent theorem, the analytic functions $u_0(\zeta)$, $\phi_0(\zeta)$, and $w_0(\zeta)$ defined in the ring region R_0 can be expressed as

$$\begin{Bmatrix} u_0(\zeta) \\ \phi_0(\zeta) \\ w_0(\zeta) \end{Bmatrix} = \begin{Bmatrix} u_0^+(\zeta) \\ \phi_0^+(\zeta) \\ w_0^+(\zeta) \end{Bmatrix} + \begin{Bmatrix} u_0^-(\zeta) \\ \phi_0^-(\zeta) \\ w_0^-(\zeta) \end{Bmatrix} \tag{28}$$

where the superscripts " + " and " − " denote that the corresponding functions are analytic in regions $|\zeta| < \gamma_2$ and $|\zeta| > \gamma_1$, respectively. Without loss of generality, it can be assumed that in agreement to Eq. (25)

$$\begin{Bmatrix} u_0^+(1) \\ \phi_0^+(1) \\ w_0^+(1) \end{Bmatrix} = \begin{Bmatrix} 0 \\ 0 \\ 0 \end{Bmatrix}, \begin{Bmatrix} u_0^-(1) \\ \phi_0^-(1) \\ w_0^-(1) \end{Bmatrix} = \begin{Bmatrix} u_0(1) \\ \phi_0(1) \\ w_0(1) \end{Bmatrix}. \tag{29}$$

By substituting Eq. (28) into (26), one can arrive at

$$2 \begin{Bmatrix} u_0^+(\zeta) \\ \phi_0^+(\zeta) \\ w_0^+(\zeta) \end{Bmatrix} - (\zeta - 1)[E_1] \begin{Bmatrix} U_1(\zeta) \\ \Phi_1(\zeta) \\ W_1(\zeta) \end{Bmatrix} = -2 \begin{Bmatrix} u_0^-(\zeta) \\ \phi_0^-(\zeta) \\ w_0^-(\zeta) \end{Bmatrix} + (\zeta + 1)[E_2] \begin{Bmatrix} \overline{U_1(\zeta)} \\ \overline{\Phi_1(\zeta)} \\ \overline{W_1(\zeta)} \end{Bmatrix} \quad (|\zeta| = \gamma_1), \tag{30}$$

$$2 \begin{Bmatrix} u_0^-(\zeta) \\ \phi_0^-(\zeta) \\ w_0^-(\zeta) \end{Bmatrix} - (\zeta - 1)[F_1] \begin{Bmatrix} U_2(\zeta) \\ \Phi_2(\zeta) \\ W_2(\zeta) \end{Bmatrix} = -2 \begin{Bmatrix} u_0^+(\zeta) \\ \phi_0^+(\zeta) \\ w_0^+(\zeta) \end{Bmatrix} + (\zeta + 1)[F_2] \begin{Bmatrix} \overline{U_2(\zeta)} \\ \overline{\Phi_2(\zeta)} \\ \overline{W_2(\zeta)} \end{Bmatrix} \quad |\zeta| = \gamma_2 \tag{31}$$

where the matrices $[\mathbf{E}_1]$, $[\mathbf{E}_2]$, $[\mathbf{F}_1]$, and $[\mathbf{F}_2]$ are defined as

$$\begin{aligned}[\mathbf{E}_1] &= [\mathbf{B}_1] + [\mathbf{B}_{01}],\ [\mathbf{E}_2] = [\mathbf{B}_1] - [\mathbf{B}_{01}],\\ [\mathbf{F}_1] &= [\mathbf{B}_2] + [\mathbf{B}_{02}],\ [\mathbf{F}_2] = [\mathbf{B}_2] - [\mathbf{B}_{02}]\end{aligned} \tag{32}$$

in which the matrices $[\mathbf{B}_1]$, $[\mathbf{B}_2]$, $[\mathbf{B}_{01}]$, and $[\mathbf{B}_{02}]$ are defined in Eq. (27).

To apply the theorem of analytic continuation to Eqs. (30) and (31), it is convenient to introduce the following analytic functions [34]:

$$F_1(\zeta) = \begin{cases} 2\begin{Bmatrix} u_0^+(\zeta)\\ \phi_0^+(\zeta)\\ w_0^+(\zeta)\end{Bmatrix} - (\zeta-1)[\mathbf{E}_1]\begin{Bmatrix} U_1(\zeta)\\ \Phi_1(\zeta)\\ W_1(\zeta)\end{Bmatrix}, (|\zeta|<\gamma_1)\\ -2\begin{Bmatrix} u_0^-(\zeta)\\ \phi_0^-(\zeta)\\ w_0^-(\zeta)\end{Bmatrix} + (\zeta+1)[\mathbf{E}_2]\begin{Bmatrix} \overline{U_1(\gamma_1^2/\bar{\zeta})}\\ \overline{\Phi_1(\gamma_1^2/\bar{\zeta})}\\ \overline{W_1(\gamma_1^2/\bar{\zeta})}\end{Bmatrix}, (|\zeta|>\gamma_1), \end{cases} \tag{33}$$

$$F_2(\zeta) = \begin{cases} 2\begin{Bmatrix} u_0^-(\zeta)\\ \phi_0^-(\zeta)\\ w_0^-(\zeta)\end{Bmatrix} - (\zeta-1)[\mathbf{F}_1]\begin{Bmatrix} U_2(\zeta)\\ \Phi_2(\zeta)\\ W_2(\zeta)\end{Bmatrix}, (|\zeta|>\gamma_2)\\ -2\begin{Bmatrix} u_0^+(\zeta)\\ \phi_0^+(\zeta)\\ w_0^+(\zeta)\end{Bmatrix} + (\zeta+1)[\mathbf{F}_2]\begin{Bmatrix} \overline{U_2(\gamma_2^2/\bar{\zeta})}\\ \overline{\Phi_2(\gamma_2^2/\bar{\zeta})}\\ \overline{W_2(\gamma_2^2/\bar{\zeta})}\end{Bmatrix}, (|\zeta|<\gamma_2). \end{cases} \tag{34}$$

By application of the Liouville theorem, one has

$$F_1(\zeta) = \{\mathbf{c}_1\} = \begin{Bmatrix} c_{11} & c_{12} & c_{13}\end{Bmatrix}^T,\ F_2(\zeta) = \{\mathbf{c}_2\} = \begin{bmatrix} c_{21} & c_{22} & c_{23}\end{bmatrix}^T \tag{35}$$

where $\mathbf{c}_1$ and $\mathbf{c}_2$ are constant column complex vectors, and the superscript "T" denotes the transpose of the corresponding matrix. From Eqs. (29), (33), and (34), the constants $\mathbf{c}_1$ and $\mathbf{c}_2$ can be determined as

$$\begin{aligned}\{\mathbf{c}_1\} &= \begin{Bmatrix} u_0(1)\\ \phi_0(1)\\ w_0(1)\end{Bmatrix} = (x_2-x_1)\begin{bmatrix} 1 & \alpha_{10} & \alpha_{20}\\ 0 & -1/\lambda_{11}^0 & 0\\ \delta_{10} & \delta_{20} & 1\end{bmatrix}^{-1}\begin{Bmatrix} \sigma_{zx}^0 - i\sigma_{zy}^0\\ E_x^0 - iE_y^0\\ H_{zx}^0 - iH_{zy}^0\end{Bmatrix},\\ \{\mathbf{c}_2\} &= \begin{bmatrix} 0 & 0 & 0\end{bmatrix}^T.\end{aligned} \tag{36}$$

It is noted that the constant terms $\mathbf{c}_1$ represent rigid body motion and equipotential field, which do not affect the deformation of the body and are therefore omitted.

Combining Eqs. (33–36), and according to the reflection principle across circles $|\zeta| = \gamma_1$ and $|\zeta| = \gamma_2$, one can obtain the following relations:

$$\begin{aligned}&2\begin{Bmatrix} u_0^+(\zeta)\\ \phi_0^+(\zeta)\\ w_0^+(\zeta)\end{Bmatrix} - (\zeta-1)[\mathbf{E}_1]\begin{Bmatrix} U_1(\zeta)\\ \Phi_1(\zeta)\\ W_1(\zeta)\end{Bmatrix} = \begin{Bmatrix} c_{11}\\ c_{12}\\ c_{13}\end{Bmatrix},\ (|\zeta|<\gamma_1),\\ &-2\begin{Bmatrix} \overline{u_0^-(\gamma_1^2/\bar{\zeta})}\\ \overline{\phi_0^-(\gamma_1^2/\bar{\zeta})}\\ \overline{w_0^-(\gamma_1^2/\bar{\zeta})}\end{Bmatrix} + \left(\frac{\gamma_1^2}{\zeta}-1\right)[\mathbf{E}_2]\begin{Bmatrix} U_1(\zeta)\\ \Phi_1(\zeta)\\ W_1(\zeta)\end{Bmatrix} = \begin{Bmatrix} \overline{c_{11}}\\ \overline{c_{12}}\\ \overline{c_{13}}\end{Bmatrix}, (|\zeta|<\gamma_1),\\ &-2\begin{Bmatrix} u_0^+(\zeta)\\ \phi_0^+(\zeta)\\ w_0^+(\zeta)\end{Bmatrix} + (\zeta-1)[\mathbf{F}_2]\begin{Bmatrix} \overline{U_2(\gamma_2^2/\bar{\zeta})}\\ \overline{\Phi_2(\gamma_2^2/\bar{\zeta})}\\ \overline{W_2(\gamma_2^2/\bar{\zeta})}\end{Bmatrix} = \begin{Bmatrix} 0\\ 0\\ 0\end{Bmatrix}, (|\zeta|<\gamma_2),\end{aligned} \tag{37}$$

$$2\begin{Bmatrix} \overline{u_0^-(\gamma_2^2/\bar{\zeta})}\\ \overline{\phi_0^-(\gamma_2^2/\bar{\zeta})}\\ \overline{w_0^-(\gamma_2^2/\bar{\zeta})}\end{Bmatrix} - \left(\frac{\gamma_2^2}{\zeta}-1\right)[\mathbf{F}_1]\begin{Bmatrix} \overline{U_2(\gamma_2^2/\bar{\zeta})}\\ \overline{\Phi_2(\gamma_2^2/\bar{\zeta})}\\ \overline{W_2(\gamma_2^2/\bar{\zeta})}\end{Bmatrix} = \begin{Bmatrix} 0\\ 0\\ 0\end{Bmatrix},\ (|\zeta|<\gamma_2). \tag{38}$$

By eliminating functions $U_1(\zeta)$, $\Phi_1(\zeta)$, and $W_1(\zeta)$ from Eq. (37), we can obtain the following relations:

$$\begin{Bmatrix} \overline{u_0^-(\gamma_1^2/\overline{\zeta})} \\ \overline{\phi_0^-(\gamma_1^2/\overline{\zeta})} \\ \overline{w_0^-(\gamma_1^2/\overline{\zeta})} \end{Bmatrix} = \frac{\gamma_1^2/\zeta - 1}{\zeta - 1}[\mathbf{E}_2][\mathbf{E}_1]^{-1} \begin{Bmatrix} u_0^+(\zeta) \\ \phi_0^+(\zeta) \\ w_0^+(\zeta) \end{Bmatrix} + [\mathbf{H}] \begin{Bmatrix} \frac{\gamma_1^2/\zeta - 1}{\zeta - 1} \\ 1 \end{Bmatrix}, (|\zeta| < \gamma_1) \tag{39}$$

where the matrix $[\mathbf{H}]$ is defined as

$$[\mathbf{H}] = \begin{bmatrix} H_1 & H_2 \\ H_3 & H_4 \\ H_5 & H_6 \end{bmatrix} = -\frac{1}{2}\left([\mathbf{E}_2][\mathbf{E}_1]^{-1} \begin{bmatrix} c_{11} & 0 \\ c_{12} & 0 \\ c_{13} & 0 \end{bmatrix} + \begin{bmatrix} 0 & \overline{c_{11}} \\ 0 & \overline{c_{12}} \\ 0 & \overline{c_{13}} \end{bmatrix} \right), \tag{40}$$

In a similar way, we can solve Eq. (38) to obtain the following relations:

$$\begin{Bmatrix} u_0^+(\zeta) \\ \phi_0^+(\zeta) \\ w_0^+(\zeta) \end{Bmatrix} = \frac{\zeta - 1}{\gamma_2^2/\zeta - 1}[\mathbf{F}_2][\mathbf{F}_1]^{-1} \begin{Bmatrix} \overline{u_0^-(\gamma_2^2/\overline{\zeta})} \\ \overline{\phi_0^-(\gamma_2^2/\overline{\zeta})} \\ \overline{w_0^-(\gamma_2^2/\overline{\zeta})} \end{Bmatrix}, \ (|\zeta| < \gamma_2). \tag{41}$$

According to the principle of analytic continuation and Eqs. (39, 41), we can solve the present problem in the region $|\zeta| < \gamma_1$. After some manipulation one can obtain the following equations:

$$\begin{Bmatrix} \overline{u_0^-(\gamma_1^2/\overline{\zeta})} \\ \overline{\phi_0^-(\gamma_1^2/\overline{\zeta})} \\ \overline{w_0^-(\gamma_1^2/\overline{\zeta})} \end{Bmatrix} = \frac{\gamma_1^2/\zeta - 1}{\gamma_2^2/\zeta - 1}[G] \begin{Bmatrix} \overline{u_0^-(\gamma_2^2/\overline{\zeta})} \\ \overline{\phi_0^-(\gamma_2^2/\overline{\zeta})} \\ \overline{w_0^-(\gamma_2^2/\overline{\zeta})} \end{Bmatrix} + [H] \begin{Bmatrix} \frac{\gamma_1^2/\zeta - 1}{\zeta - 1} \\ 1 \end{Bmatrix} \quad (|\zeta| < \gamma_1) \tag{42}$$

where the matrix $[\mathbf{G}]$ is defined as

$$[\mathbf{G}] = [\mathbf{E}_2][\mathbf{E}_1]^{-1}[\mathbf{F}_2][\mathbf{F}_1]^{-1}. \tag{43}$$

Applying the reflection principle across the circle $|\zeta| = \gamma_1$ to Eq. (42) leads to the following expression:

$$\begin{Bmatrix} u_0^-(\zeta) \\ \phi_0^-(\zeta) \\ w_0^-(\zeta) \end{Bmatrix} = \frac{\zeta - 1}{\Gamma^{-2}\zeta - 1}[G] \begin{Bmatrix} u_0^-(\Gamma^{-2}\zeta) \\ \phi_0^-(\Gamma^{-2}\zeta) \\ w_0^-(\Gamma^{-2}\zeta) \end{Bmatrix} + \left[\overline{H}\right] \begin{Bmatrix} \frac{\zeta(\zeta-1)}{\gamma_1^2 - \zeta} \\ 1 \end{Bmatrix} \quad (|\zeta| > \gamma_1) \tag{44}$$

where $\Gamma = \gamma_1/\gamma_2 < 1$ and $\left[\overline{\mathbf{H}}\right]$ is the conjugate of the matrix $[\mathbf{H}]$.

It is noted that Eqs. (44) are the functional equations to determine the unknown functions $u_0^-(\zeta)$, $\phi_0^-(\zeta)$ and $w_0^-(\zeta)$. The sequential transformations in region $|\zeta| > \gamma_1$ are adopted to solve these functions, and the results are

$$\begin{Bmatrix} u_0^-(\zeta) \\ \phi_0^-(\zeta) \\ w_0^-(\zeta) \end{Bmatrix} = \frac{\zeta - 1}{\Gamma^{-2(n+1)}\zeta - 1}[G]^{n+1} \begin{Bmatrix} u_0^-(\Gamma^{-2(n+1)}\zeta) \\ \phi_0^-(\Gamma^{-2(n+1)}\zeta) \\ w_0^-(\Gamma^{-2(n+1)}\zeta) \end{Bmatrix} + \sum_{k=0}^{n} [G]^k \left[\overline{H}\right] \begin{Bmatrix} \frac{\zeta(\zeta-1)}{\gamma_1^2\Gamma^{2k} - \zeta} \\ \frac{\zeta - 1}{\Gamma^{-2k}\zeta - 1} \end{Bmatrix} \quad (|\zeta| > \gamma_1). \tag{45}$$

If the terms $\Gamma^{2(n+1)} \begin{Bmatrix} u_0^-(\Gamma^{-2(n+1)}\zeta) \\ \phi_0^-(\Gamma^{-2(n+1)}\zeta) \\ w_0^-(\Gamma^{-2(n+1)}\zeta) \end{Bmatrix}$ are bounded and $\lim_{n\to\infty}[\mathbf{G}]^n = \begin{bmatrix} 0 & 0 & 0 \\ 0 & 0 & 0 \\ 0 & 0 & 0 \end{bmatrix}$, then the first term on the right-hand side of Eq. (45) vanishes when $n \to \infty$, and Eq. (45) can be rewritten as

$$\begin{Bmatrix} u_0^-(\zeta) \\ \phi_0^-(\zeta) \\ w_0^-(\zeta) \end{Bmatrix} = (\zeta - 1)\sum_{k=0}^{\infty} [G]^k \left[\overline{H}\right] \begin{Bmatrix} \frac{\zeta}{\gamma_1^2\Gamma^{2k} - \zeta} \\ \frac{1}{\Gamma^{-2k}\zeta - 1} \end{Bmatrix} \quad (|\zeta| > \gamma_1). \tag{46}$$

The substitution of Eq. (46) into Eq. (41) yields

$$\begin{Bmatrix} u_0^+(\zeta) \\ \phi_0^+(\zeta) \\ w_0^+(\zeta) \end{Bmatrix} = (\zeta - 1)[F_2][F_1]^{-1} \sum_{k=0}^{\infty} [G]^k [H] \begin{Bmatrix} \frac{1}{\Gamma^{2(k+1)}\zeta - 1} \\ \frac{\Gamma^{2k}\zeta}{\gamma_2^2 - \Gamma^{2k}\zeta} \end{Bmatrix} \quad (|\zeta| < \gamma_2). \tag{47}$$

Combining Eqs. (24, 28, 46, 47), the corresponding complex analytical functions in regions R_0, R_1, and R_2 can be determined as follows:

$$\begin{Bmatrix} U_0(\zeta) \\ \Phi_0(\zeta) \\ W_0(\zeta) \end{Bmatrix} = \frac{1}{\zeta - 1} \begin{Bmatrix} u_0^+(\zeta) + u_0^-(\zeta) \\ \phi_0^+(\zeta) + \phi_0^-(\zeta) \\ w_0^+(\zeta) + w_0^-(\zeta) \end{Bmatrix} \quad (\gamma_1 < |\zeta| < \gamma_2), \tag{48}$$

$$\begin{Bmatrix} U_1(\zeta) \\ \Phi_1(\zeta) \\ W_1(\zeta) \end{Bmatrix} = \frac{2}{\zeta - 1} [E_1]^{-1} \begin{Bmatrix} u_0^+(\zeta) + u_0(1) \\ \phi_0^+(\zeta) + \phi_0(1) \\ w_0^+(\zeta) + w_0(1) \end{Bmatrix} \quad (|\zeta| < \gamma_1), \tag{49}$$

$$\begin{Bmatrix} U_2(\zeta) \\ \Phi_2(\zeta) \\ W_2(\zeta) \end{Bmatrix} = \frac{2}{\zeta - 1} [F_1]^{-1} \begin{Bmatrix} u_0^-(\zeta) \\ \phi_0^-(\zeta) \\ w_0^-(\zeta) \end{Bmatrix} \quad |(\zeta| > \gamma_2). \tag{50}$$

After these complex potential functions are obtained, the mechanical and electrical fields in the transformed domain can be calculated using the relations shown in Eqs. (12–14). The mechanical and electrical fields in the composite material depend on the material constants of the circular inclusions and matrix, geometric parameters of the composite system, and the applied loadings at infinity. If the inverse transformation of Eq. (10) is applied, one can easily obtain the corresponding fields in the original plane.

It is to be noted that if the phason field is not considered, the solution obtained can be reduced to the result for a piezoelectric composite with two circular cylindrical inclusions [29]. If the piezoelectric effect of the material disappears, the solution can be further reduced to the result of two circular inclusions in an elastic medium [23, 24, 35].

4 Electro-elastic field solutions

The substitution of the complex potentials of Eqs. (48–50) into Eqs. (12–14) leads to the complete solutions of the displacements, electric potential, stresses, and electric displacements of the matrix and inclusions in the transformed plane (ζ-plane). The antiplane shear stresses in phonon and phason fields and electric displacements in the transformed plane can be obtained as follows:

$$\begin{Bmatrix} \sigma_{zx} - i\sigma_{zy} \\ D_x - iD_y \\ H_{zx} - iH_{zy} \end{Bmatrix} = \frac{(\zeta - 1)^2}{(x_1 - x_2)} [A_0] \frac{\partial}{\partial \zeta} \begin{Bmatrix} U_0(\zeta) \\ \Phi_0(\zeta) \\ W_0(\zeta) \end{Bmatrix} \quad (\gamma_1 < |\zeta| < \gamma_2), \tag{51}$$

$$\begin{Bmatrix} \sigma_{zx} - i\sigma_{zy} \\ D_x - iD_y \\ H_{zx} - iH_{zy} \end{Bmatrix} = \frac{(\zeta - 1)^2}{(x_1 - x_2)} [A_1] \frac{\partial}{\partial \zeta} \begin{Bmatrix} U_1(\zeta) \\ \Phi_1(\zeta) \\ W_1(\zeta) \end{Bmatrix} \quad (|\zeta| < \gamma_1), \tag{52}$$

$$\begin{Bmatrix} \sigma_{zx} - i\sigma_{zy} \\ D_x - iD_y \\ H_{zx} - iH_{zy} \end{Bmatrix} = \frac{(\zeta - 1)^2}{(x_1 - x_2)} [A_2] \frac{\partial}{\partial \zeta} \begin{Bmatrix} U_2(\zeta) \\ \Phi_2(\zeta) \\ W_2(\zeta) \end{Bmatrix} \quad (|\zeta| > \gamma_2) \tag{53}$$

where

$$\frac{\partial}{\partial\zeta}\begin{Bmatrix} U_0(\zeta) \\ \Phi_0(\zeta) \\ W_0(\zeta) \end{Bmatrix} = \sum_{k=0}^{\infty}[G]^k\big[\overline{H}\big]\begin{Bmatrix} \frac{\gamma_1^2\Gamma^{2k}}{(\gamma_1^2\Gamma^{2k}-\zeta)^2} \\ \frac{-\Gamma^{-2k}}{(\Gamma^{2k}-\zeta)^2} \end{Bmatrix} + [F_2][F_1]^{-1}\sum_{k=0}^{\infty}[G]^k[H]\begin{Bmatrix} \frac{-\Gamma^{2(k+1)}}{(\Gamma^{2(k+1)}\zeta-1)^2} \\ \frac{\gamma_2^2\Gamma^{2k}}{(\Gamma^{2k}\zeta-\gamma_2^2)^2} \end{Bmatrix} \quad (\gamma_1 < |\zeta| < \gamma_2), \tag{54}$$

$$\frac{\partial}{\partial\zeta}\begin{Bmatrix} U_1(\zeta) \\ \Phi_1(\zeta) \\ W_1(\zeta) \end{Bmatrix} = 2[E_1]^{-1}\left([F_2][F_1]^{-1}\sum_{k=0}^{\infty}[G]^k[H]\begin{Bmatrix} \frac{-\Gamma^{2(k+1)}}{(\Gamma^{2(k+1)}\zeta-1)^2} \\ \frac{\gamma_2^2\Gamma^{2k}}{(\Gamma^{2k}\zeta-\gamma_2^2)^2} \end{Bmatrix} - \frac{1}{(\zeta-1)^2}\begin{Bmatrix} u_0(1) \\ \phi_0(1) \\ w_0(1) \end{Bmatrix}\right) \quad |\zeta| < \gamma_1, \tag{55}$$

$$\frac{\partial}{\partial\zeta}\begin{Bmatrix} U_2(\zeta) \\ \Phi_2(\zeta) \\ W_2(\zeta) \end{Bmatrix} = 2[F_1]^{-1}\sum_{k=0}^{\infty}[G]^k\big[\overline{H}\big]\begin{Bmatrix} \frac{\gamma_1^2\Gamma^{2k}}{(\gamma_1^2\Gamma^{2k}-\zeta)^2} \\ \frac{-\Gamma^{-2k}}{(\Gamma^{2k}-\zeta)^2} \end{Bmatrix} \quad (|\zeta| > \gamma_2), \tag{56}$$

and the matrices $[\mathbf{A}_0]$, $[\mathbf{A}_1]$, and $[\mathbf{A}_2]$ are defined from Eq. (20) as

$$\big[A_j\big] = \begin{bmatrix} 1 & \alpha_{1j} & \alpha_{2j} \\ \mu_{1j} & -1 & \mu_{2j} \\ \delta_{1j} & \delta_{2j} & 1 \end{bmatrix} \quad (j = 0, 1, 2). \tag{57}$$

From Eqs. (51–57), it can be observed that the electro-elastic fields depend on the material constants of the individual phases of the inclusions and the matrix, the geometric parameters of the composite system, and the mechanical and electrical loading applied at infinity. The corresponding stress and electric displacement fields in the original z-plane can be obtained by applying the inverse transformation of Eqs. (10–11).

5 Validation of the model

In this Section, we examine some interesting cases which demonstrate the validity and versatility of the obtained formulations.

5.1 Unified material for inclusion-1 and matrix

When the inclusion-1 (in regions 1) and the matrix (in region 0) are of the same material, while inclusion-2 is of a different material, we can get the special case of a homogeneous 1D piezoelectric QC material with a circular cylindrical inhomogeneity under antiplane shear and inplane electric loadings. For this special crack problem, we have

$$\begin{aligned} &c_{44}^0 = c_{44}^1,\ \ \lambda_{11}^0 = \lambda_{11}^1,\ \ K_2^0 = K_2^1, \\ &[\mathbf{A}_1] = [\mathbf{A}_0],\ \ [\mathbf{B}_{01}] = [\mathbf{A}_0]^{-1}[\mathbf{A}_1] = [\mathbf{I}] = [\mathbf{B}_1], \\ &[\mathbf{E}_1] = [\mathbf{B}_1] + [\mathbf{B}_{01}] = 2[\mathbf{I}],\ [\mathbf{E}_2] = [\mathbf{B}_1] - [\mathbf{B}_{01}] = [\mathbf{0}], \\ &[\mathbf{G}] = [\mathbf{E}_2][\mathbf{E}_1]^{-1}[\mathbf{F}_2][\mathbf{F}_1]^{-1} = [\mathbf{0}],\ \ [\mathbf{H}] = -\frac{1}{2}\big[\mathbf{0}\ \overline{\mathbf{c}_1}\big] \end{aligned} \tag{58}$$

where $[\mathbf{I}]$ and $[\mathbf{0}]$ are the identity matrix and zero matrix, respectively.

The antiplane shear stresses in phonon and phason fields and electric fields in the transformed plane can be obtained as

$$\begin{Bmatrix} \sigma_{zx} - i\sigma_{zy} \\ E_x - iE_y \\ H_{zx} - iH_{zy} \end{Bmatrix} = \begin{Bmatrix} \sigma^0_{zx} - i\sigma^0_{zy} \\ E^0_x - iE^0_y \\ H^0_{zx} - iH^0_{zy} \end{Bmatrix} - \frac{\gamma_2^2(\zeta-1)^2}{(\gamma_2^2-\zeta^2)}[M_0][F_2][F_1]^{-1}[M_0]^{-1} \begin{Bmatrix} \sigma^0_{zx} + i\sigma^0_{zy} \\ E^0_x + iE^0_y \\ H^0_{zx} + iH^0_{zy} \end{Bmatrix} \quad (|\zeta| \le \gamma_2), \tag{59}$$

$$\begin{Bmatrix} \sigma_{zx} - i\sigma_{zy} \\ E_x - iE_y \\ H_{zx} - iH_{zy} \end{Bmatrix} = [M_2][M_0]^{-1} \begin{Bmatrix} \sigma^0_{zx} - i\sigma^0_{zy} \\ E^0_x - iE^0_y \\ H^0_{zx} - iH^0_{zy} \end{Bmatrix} \quad (|\zeta| \ge \gamma_2) \tag{60}$$

where the matrices $[\mathbf{M}_j]$ $(j = 0, 1, 2)$ are defined as

$$[M_j] = \begin{bmatrix} 1 & \alpha_{1j} & \alpha_{2j} \\ 0 & -1/\lambda^{(j)}_{11} & 0 \\ \delta_{1j} & \delta_{2j} & 1 \end{bmatrix} \quad (j = 0, 1, 2) \tag{61}$$

and the constants α_{1j}, α_{2j}, δ_{1j} and δ_{2j} $(j = 0, 1, 2)$ are defined in Eq. (22).

It can be observed from Eqs. (59) and (60) that the electro-mechanical field in the matrix $(|\zeta| \le \gamma_2)$ consists of two parts: the first part is the homogeneous field which is equal to the far-field loading, and the second part is the perturbed field due to the existence of the circular inclusion. The electro-mechanical fields inside the circular inclusion are constant fields, which depend on the material properties of the matrix and inclusion, and the loadings applied at infinity.

If we further assume that inclusion-2 has the same material properties as the matrix, i.e.,

$$\begin{aligned} &c^2_{44} = c^0_{44} = c^1_{44}, \ \ \lambda^2_{11} = \lambda^0_{11} = \lambda^1_{11}, \ \ K^2_2 = K^0_2 = K^1_2, \\ &[\mathbf{A}_2] = [\mathbf{A}_0], \ \ [\mathbf{B}_{02}] = [\mathbf{A}_0]^{-1}[\mathbf{A}_2] = [\mathbf{I}] = [\mathbf{B}_2], \\ &[\mathbf{M}_2] = [\mathbf{M}_1] = [\mathbf{M}_0], \\ &[\mathbf{F}_1] = [\mathbf{B}_2] + [\mathbf{B}_{02}] = 2[\mathbf{I}], \ \ [\mathbf{F}_2] = [\mathbf{B}_2] - [\mathbf{B}_{02}] = [\mathbf{0}], \end{aligned} \tag{62}$$

then, the substitution of Eq. (62) into Eq. (59) and (60) leads to the constant/homogeneous fields in a homogeneous medium under uniform loadings at infinity; viz.,

$$\begin{Bmatrix} \sigma_{zx} - i\sigma_{zy} \\ E_x - iE_y \\ H_{zx} - iH_{zy} \end{Bmatrix} = \begin{Bmatrix} \sigma^0_{zx} - i\sigma^0_{zy} \\ E^0_x - iE^0_y \\ H^0_{zx} - iH^0_{zy} \end{Bmatrix} \quad (|\zeta| \ge 0). \tag{63}$$

5.2 Circular inclusions replaced by cavities

When the two circular cylindrical inclusions are replaced by cavities, the continuity conditions of displacements, electric potential, tractions, and normal component of electric displacement along the interface can be simplified, and similar solving steps could be adopted. In this case, Eq. (20) can be rewritten as follows:

$$\begin{bmatrix} 1 & \alpha_{10} & \alpha_{20} \\ \mu_{10} & -1 & \mu_{20} \\ \delta_{10} & \delta_{20} & 1 \end{bmatrix} \begin{Bmatrix} \mathrm{Im}[U_0(\zeta)] \\ \mathrm{Im}[\Phi_0(\zeta)] \\ \mathrm{Im}[W_0(\zeta)] \end{Bmatrix} = \begin{Bmatrix} 0 \\ 0 \\ 0 \end{Bmatrix} \quad |\zeta| = \gamma_j \tag{64}$$

which indicates that the tractions and the normal component of the electric displacement along the free surface are equal to zero.

Direct numerical calculation for the case of diminishing material properties of the inclusions (compared to those of the matrix) may be performed to simulate the presence of cylindrical cavities in an infinite matrix.

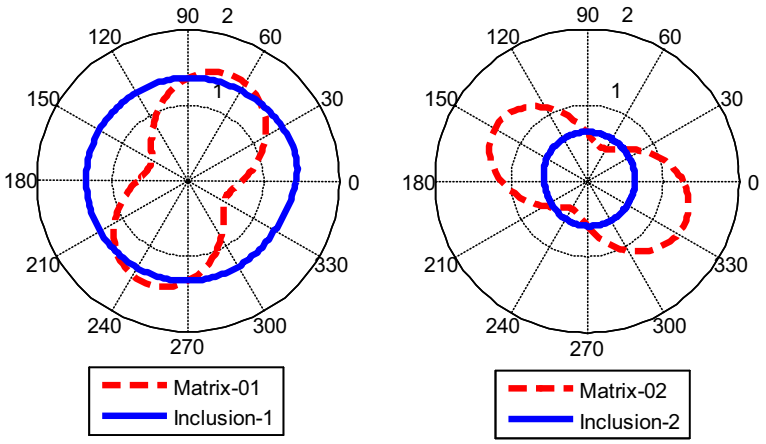

Fig. 3 Normalized shear stress σ_{zy}/P_0 along interfaces 1 and 2, when $\sigma^0_{zy} = \sigma^0_{zx} = P_0$

5.3 Rigid circular inclusions

When the material properties of the two circular cylindrical inclusions are close to infinity, the continuity conditions of displacements, electric potential, tractions, and normal component of electric displacement along the interface can be simplified. In this case, $\beta_{1j} = \beta_{2j} = \beta_{3j} = 0$, $(j = 1, 2)$, $[\mathbf{B}_1] = [\mathbf{B}_2] = [\mathbf{0}]$, and Eq. (19) can be rewritten as

$$\begin{Bmatrix} U_0(\zeta) \\ \Phi_0(\zeta) \\ W_0(\zeta) \end{Bmatrix} + \begin{Bmatrix} \overline{U_0(\zeta)} \\ \overline{\Phi_0(\zeta)} \\ \overline{W_0(\zeta)} \end{Bmatrix} = \begin{Bmatrix} 0 \\ 0 \\ 0 \end{Bmatrix}, \ (|\zeta| = \gamma_j) \tag{65}$$

which means that the displacements and electric potential along the interface between the rigid inclusions and matrix are equal to zero.

Direct numerical determination of the case of very large material properties of the inclusions (compared to those of the matrix) may be performed to simulate the effect of the presence of rigid circular cylindrical inclusions in an infinite matrix.

5.4 Piezoelectric composite

In this case, the quasicrystal constants are equal to zero, i.e., $R^j_3 = d^j_{15} = 0$, $(j = 0, 1, 2)$, we then have

$$\begin{aligned} &\alpha_{2j} = \delta_{1j} = \delta_{2j} = 0, \\ &[A_j] = \begin{bmatrix} 1 & \alpha_{1j} & 0 \\ \mu_{1j} & -1 & \mu_{2j} \\ 0 & 0 & 1 \end{bmatrix}, \\ &[B_{01}] = [A_0]^{-1}[A_1], \ [B_{02}] = [A_0]^{-1}[A_2] \quad (j = 0, 1, 2). \end{aligned} \tag{66}$$

5.5 Quasicrystal composite

In this case, the piezoelectric constants are equal to zero, i.e., $e^j_{15} = d^j_{15} = 0$, $(j = 0, 1, 2)$, we then have

$$\alpha_{1j} = \mu_{1j} = \mu_{2j} = 0 \quad (j = 0, 1, 2). \tag{67}$$

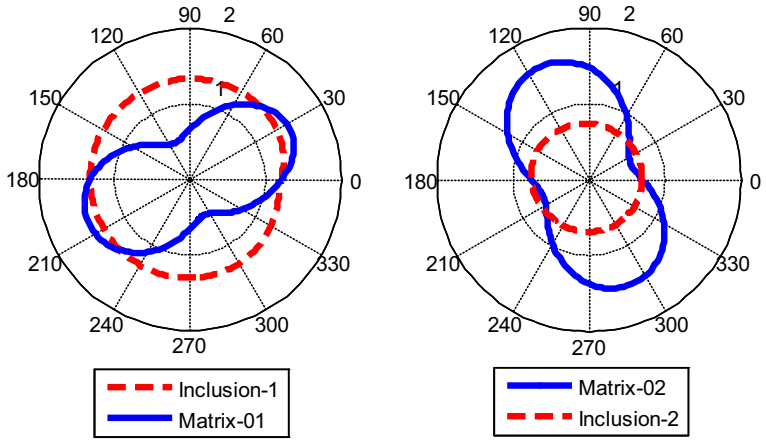

Fig. 4 Normalized shear stress σ_{zx}/P_0 along the interfaces 1 and 2, when $\sigma_{zy}^0 = \sigma_{zx}^0 = P_0$

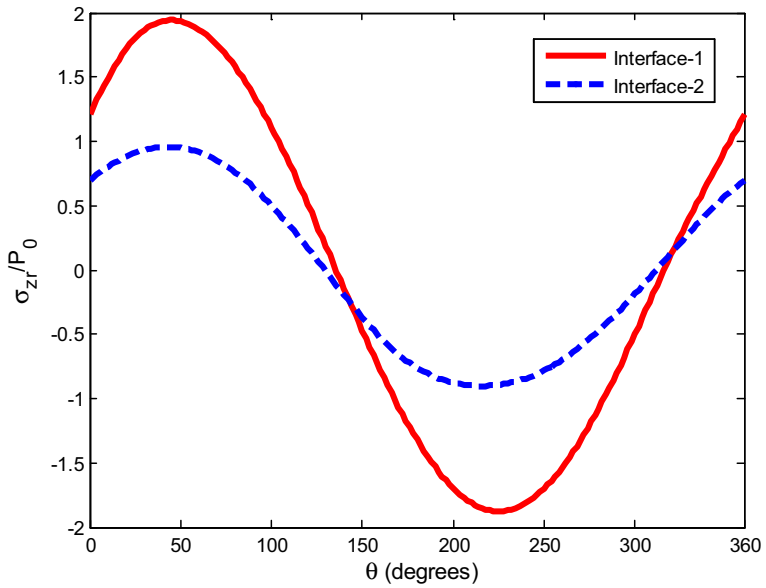

Fig. 5 Normalized radial shear stress σ_{zr}/P_0 along interfaces 1 and 2, when $\sigma_{zy}^0 = \sigma_{zx}^0 = P_0$, $h/r_1 = 2$, $r_2/r_1 = 0.5$

5.6 Purely elastic composite

In this case, the piezoelectric constants and quasicrystal constants are equal to zero, i.e., $e_{15}^j = d_{15}^j = R_3^j = 0$, $(j = 0, 1, 2)$, we then have

$$\alpha_{1j} = \alpha_{2j} = \mu_{1j} = \mu_{2j} = \delta_{1j} = \delta_{2j} = 0 \quad (j = 0, 1, 2). \tag{68}$$

6 Examples and discussions

In this Section, some examples are given to illustrate the application of the solutions obtained. The material properties of the 1D piezoelectric QC material used in the following numerical calculation for the matrix are taken from [19] as follows:

$$\begin{aligned} &c_{44} = 70.19\,\text{GPa}, \quad e_{15} = -0.138\,(\text{C}/\text{m}^2), \quad K_2 = 56\,\text{GPa}, \\ &R_3 = 15.36\,\text{GPa}, \quad d_{15} = -0.16\,(\text{C}/\text{m}^2), \quad \lambda_{11} = 8.26 \times 10^{-11}(\text{C}^2/\text{Nm}^2), \end{aligned} \tag{69}$$

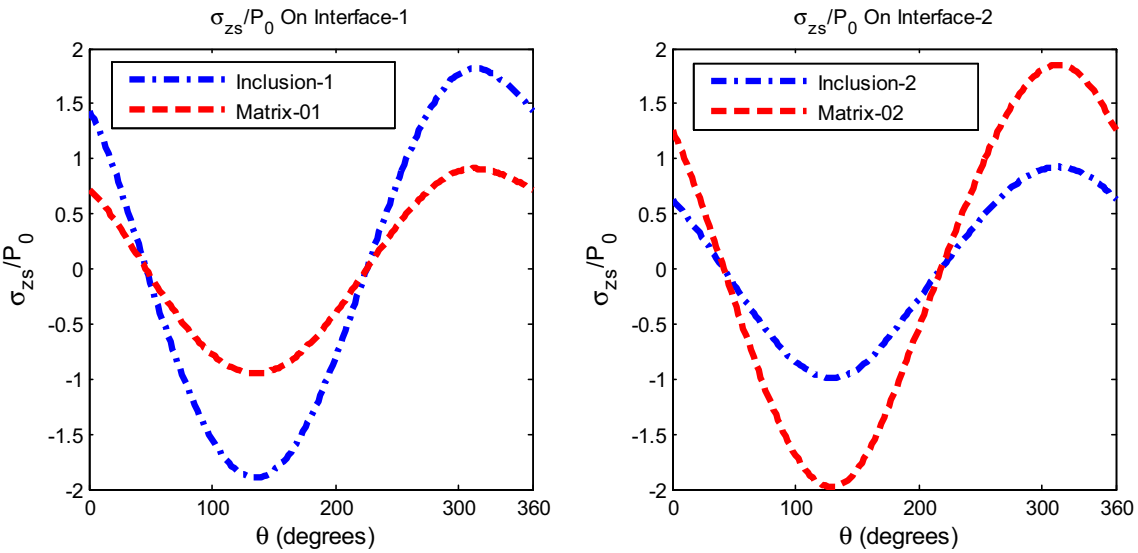

Fig. 6 Normalized tangential shear stress σ_{zs}/P_0 along interfaces 1 and 2, when $\sigma_{zy}^0 = \sigma_{zx}^0 = P_0$, $h/r_1 = 2$, $r_2/r_1 = 0.5$

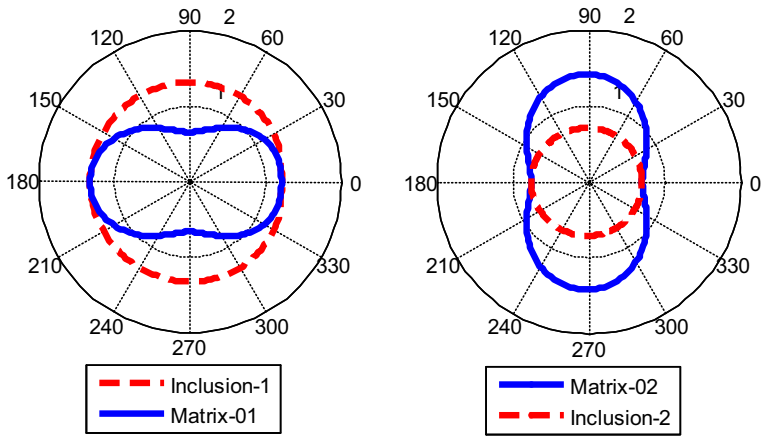

Fig. 7 Normalized shear stress σ_{zx}/P_0 along interfaces 1 and 2, when $\sigma_{zx}^0 = P_0$, $\sigma_{zy}^0 = 0$

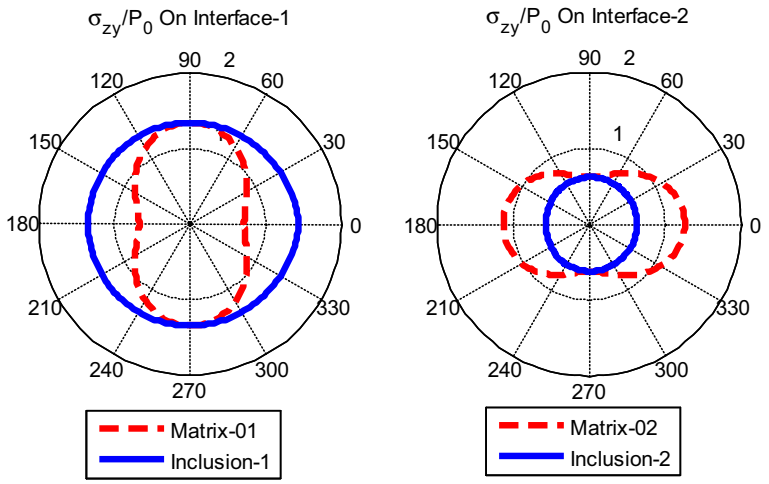

Fig. 8 Normalized shear stress σ_{zy}/P_0 along interfaces 1 and 2, when $\sigma_{zy}^0 = P_0$, $\sigma_{zx}^0 = 0$

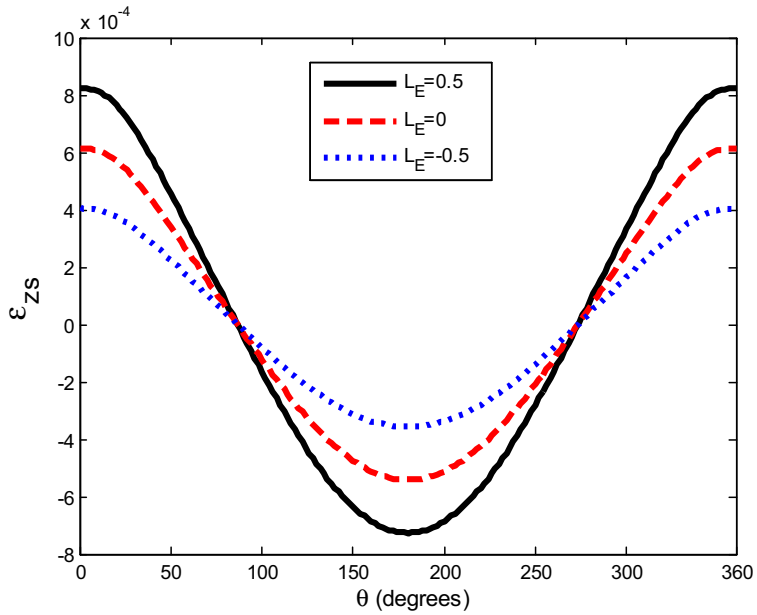

Fig. 9 Tangential shear strain ε_{zs} along interfaces 1 against θ for different electric loading parameters $L_E = e_{15}^0 E_0 / P_0$ and $P_0 = 50\,\text{MPa}$

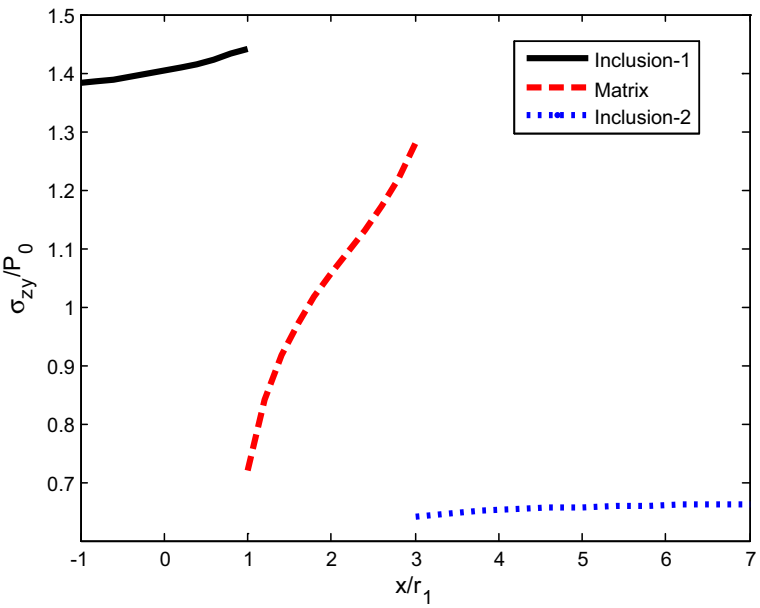

Fig. 10 Normalized shear stresses σ_{zy} / P_0 along the x-axis, when $\rho^{(1)} = 2$, $\rho^{(2)} = 0.5$ and $h / r_1 = 5$, $r_2 = 2r_1$

and the two circular cylindrical inclusions may have different material properties which are expressed as

$$M_{ij}^{(1)} = \rho^{(1)} M_{ij}^{(0)}, \quad M_{ij}^{(2)} = \rho^{(2)} M_{ij}^{(0)} \tag{70}$$

where $M_{ij}^{(0)}$ are the corresponding material constants of the matrix, as shown in Eq. (69). When the ratio number $\rho^{(1)}$ or $\rho^{(2)}$ is close to zero, the corresponding inclusion becomes a circular cylindrical cavity, and when the ratio number $\rho^{(1)}$ or $\rho^{(2)}$ is infinitely large, the circular cylindrical inclusion becomes rigid. In the special case when $\rho^{(1)} = \rho^{(2)} = 1$, the composite system becomes a homogeneous medium.

Figures 3 and 4 show the variations of the normalized stresses σ_{zy} / P_0 and σ_{zx} / P_0 along the interface between inclusion and matrix, respectively, when $h / r_1 = 2$, $r_2 / r_1 = 0.5$, $\rho^{(1)} = 2$, $\rho^{(2)} = 0.5$, and $\sigma_{zy}^0 =$

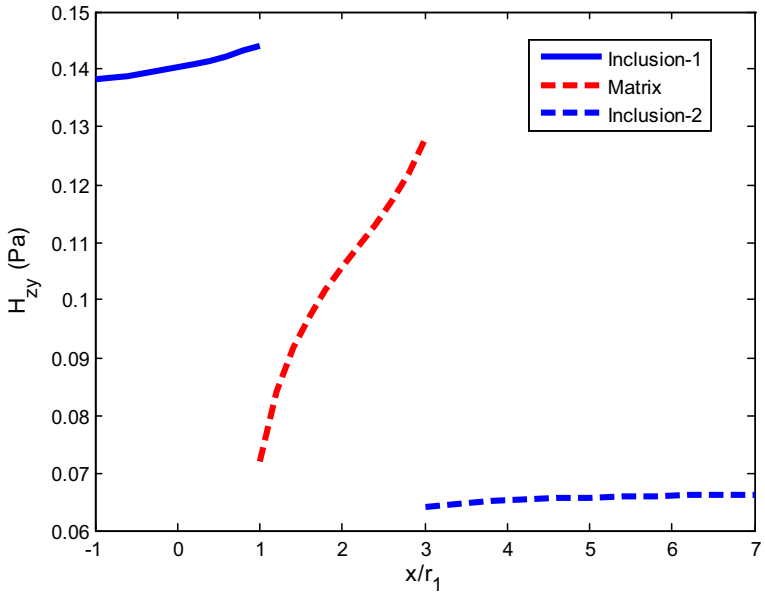

Fig. 11 Phason shear stresses H_{zy} along the x-axis, when $\rho^{(1)} = 2$, $\rho^{(2)} = 0.5$, $h/r_1 = 5$, $r_2 = 2r_1$, and $H^0_{zy} = 0.1\,Pa$

$\sigma^0_{zx} = P_0$. The plots using polar coordinates of the angle θ, in radians, and the radius show the magnitude of the normalized stresses σ_{zy}/P_0 or σ_{zx}/P_0. It is observed that the shear stresses σ_{zy} on the interface in the matrix and inclusion are different except at the angles $\theta = \pi/2$ and $\theta = 3\pi/2$; shear stresses σ_{zx} on the interface in the matrix and inclusion are different except at the angles $\theta = 0$ and $\theta = \pi$. This result is consistent with the boundary condition of traction continuity across the interface between the matrix and the inclusions ($\sigma_{zr} = \sigma_{zy}\sin(\theta) + \sigma_{zx}\cos(\theta)$). The shear stresses σ_{zy} and σ_{zx} on the interface in the inclusion with higher material ratio $\rho^{(1)} = 2$ are larger than those on the interface in the inclusion with lower material ratio $\rho^{(2)} = 0.5$.

Figure 5 shows the normalized radial shear stresses σ_{zr}/P_0 along the interfaces 1 and 2. It is observed that the stresses σ_{zr} vary with the angle θ along the interfaces between the matrix and the inclusions, and that the magnitude of the shear stresses σ_{zr} along interface 1 is larger than of that which exists along interface 2 due to the fact that $\rho^{(1)} > \rho^{(2)}$. The variation of the normalized tangential shear stresses σ_{zs}/P_0 along the interfaces 1 and 2 is displayed in Fig. 6. It is seen that the tangential stresses σ_{zs} are not continuous across the interface between matrix and inclusion except at some particular angles. Furthermore, the magnitude of the shear stresses σ_{zs} along interface 1 in the inclusion is larger than that in the matrix due to the fact that $\rho^{(1)} = 2$, and the shear stresses σ_{zs} along the interface 2 in the inclusion are smaller than that in the matrix due to the fact that $\rho^{(2)} = 0.5$.

Figures 7 and 8 depict the variation of the normalized stresses along interfaces 1 and 2 for σ_{zx}/P_0 when $\sigma^0_{zx} = P_0$, $\sigma^0_{zy} = 0$, and σ_{zy}/P_0 when $\sigma^0_{zy} = P_0$, $\sigma^0_{zx} = 0$, respectively. It is seen from Fig. 7 that the shear stress σ_{zx} in the inclusion ($\rho^{(1)} = 2$) along the interface 1 is larger than that in the matrix except that they are in the same directions when $\theta = 0$ and $\theta = \pi$. The shear stress σ_{zx} in the inclusion ($\rho^{(1)} = 0.5$) along the interface 2 is smaller than that in the matrix except that they are the same at the directions $\theta = 0$ and $\theta = \pi$. Similar results can be observed from Fig. 8 except that the interface shear stresses σ_{zy} in the matrix and inclusions 1 and 2 are the same along the directions $\theta = \pi/2$ and $\theta = 3\pi/2$.

Figure 9 depicts the tangential shear strains ε_{zs} along interface 1 at different electric loadings $L_E = e^0_{15}E_0/P_0$ when $\sigma^0_{zy} = P_0 = 50$MPa. The tangential shear strains ε_{zs} are continuous across the interface between matrix and inclusion, which indicates that the perfect bonding condition holds on the interface. It is observed that positive electric loading leads to higher magnitude of the shear strain and negative electric loading leads to lower magnitude.

Figure 10 shows the variations of the normalized shear stresses σ_{zy}/P_0 along the x-axis when $\rho^{(1)} = 2$, $\rho^{(2)} = 0.5$, $h/r_1 = 5$, $r_2 = 2r_1$, and $\sigma^0_{zy} = P_0 = 50$MPa. The discontinuity of stress σ_{zy} across the interface is displayed, and the stress in inclusion-1 ($\rho^{(1)} = 2$) is higher than that in the inclusion-2 ($\rho^{(2)} = 0.5$), and

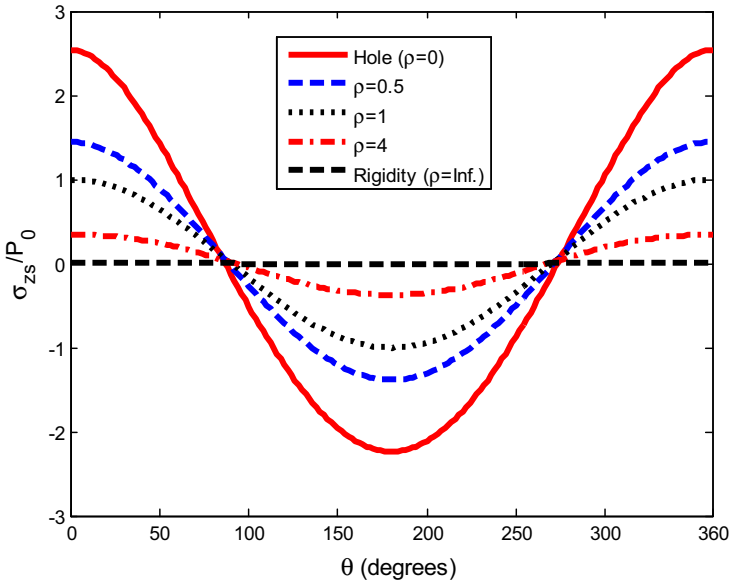

(a) Normalized shear stress the matrix acting at interfacel against θ, when $\rho^{(1)} = \rho^{(2)} = \rho$ and $h/r_1 = 5,\ r_2 = 2r_1$.

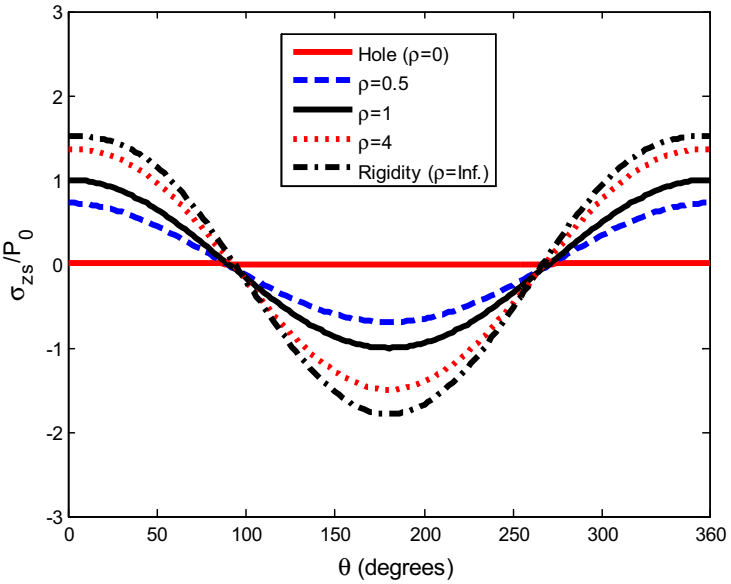

(b) Normalized shear stress in inclusion acting at interface-1, when $\rho^{(1)} = \rho^{(2)} = \rho$ and $h/r_1 = 5,\ r_2 = 2r_1$.

Fig. 12 a Normalized shear stress in the matrix acting at interface 1 against θ, when $\rho^{(1)} = \rho^{(2)} = \rho$ and $h/r_1 = 5, r_2 = 2r_1$. **b** Normalized shear stress in the inclusion acting at interface 1, when $\rho^{(1)} = \rho^{(2)} = \rho$ and $h/r_1 = 5, r_2 = 2r_1$

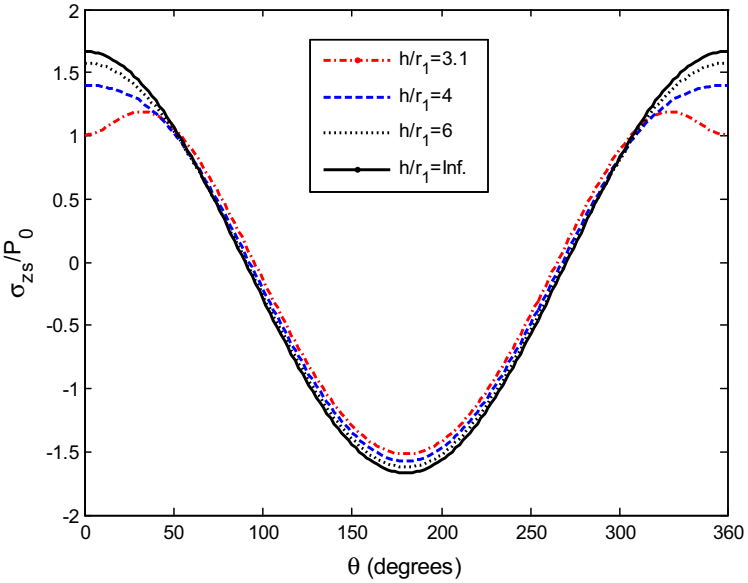

(a) Normalized shear stress the matrix at interface-1 versus θ for different normalized distances h/r_1.

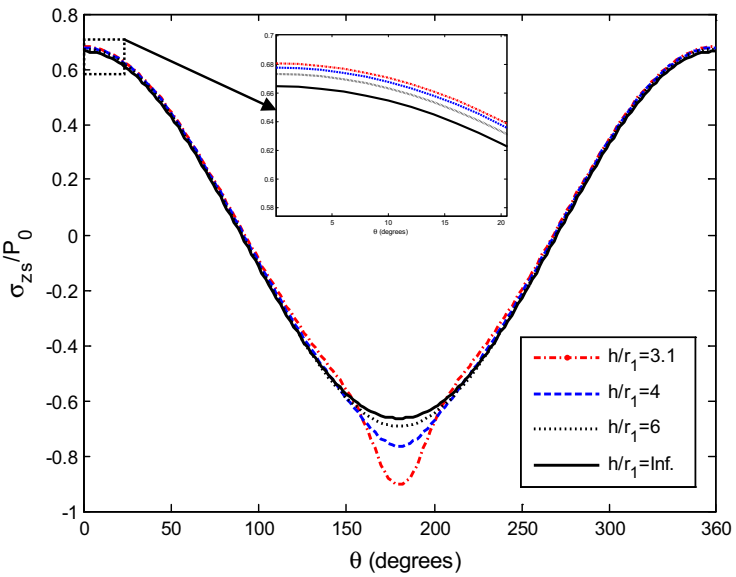

(b) Normalized shear stress in matrix at interface-2 versus θ for different normalized distances h/r_1.

Fig. 13 a Normalized shear stress in the matrix at interface 1 versus θ for different normalized distances h/r_1.**b** Normalized shear stress in the matrix at interface 2 versus θ for different normalized distances h/r_1

the stress in the matrix lies between those in the inclusions 1 and 2. This result is in agreement with Wu [24] for the case of two circular cylindrical inhomogeneities under antiplane shear loading. A similar distribution of the phason shear stress H_{zy} along the x-axis is displayed in Fig. 11, and there is discontinuity across the interfaces between matrix and inclusions.

The normalized tangential shear stresses σ_{zs}/P_0 in the matrix and inclusion on interface 1 are shown in Fig. 12a and b when $\rho^{(1)} = \rho^{(2)} = \rho$, $h/r_1 = 5$, $r_2 = 2r_1$, and $\sigma^0_{zy} = P_0 = 50\,\text{MPa}$. Figure 12a shows that, as the material ratio ρ increases from zero to infinity, the magnitude of the tangential shear stresses σ_{zs} on the interface in the matrix decreases from a particular value to zero. The limiting case of two holes ($\rho = 0$) in the

matrix is in agreement with the results of Honein et al. [23], and the result for the limiting case of two rigid inclusions in the matrix is the same as the exact solution obtained by Zhang and Hasebe [36]. The tangential shear stresses σ_{zs} on the interface in the inclusion increase from zero as the material ratio ρ increases from zero to infinity, as shown in Fig. 12b. It is observed from Fig. 12a and b that only when $\rho = 1$, i.e., the inclusion and matrix are of the same material, the tangential shear stresses σ_{zs} across the interface are continuous.

The effects of the distance h between the two circular inclusions on the tangential shear stresses on the interface 1 and interface 2 are depicted in Fig. 13a and b when $r_2/r_1 = 2$, $\rho^{(1)} = 2$, $\rho^{(2)} = 0.5$, and $\sigma^0_{zy} = P_0$. As the value of h/r_1 increases, the magnitude of the tangential shear stresses σ_{zs} in the matrix on interface 1 increases, i.e., as the distance between the two inclusions becomes larger, the magnitude of the tangential shear stresses σ_{zs} in the matrix on interface around inclusion-1 ($\rho^{(1)} = 2$) becomes larger, see Fig. 13a. Figure 13b shows the variation of the tangential shear stresses σ_{zs} in the matrix on interface 2 around inclusion-2 ($\rho^{(2)} = 0.5$), which shows that the larger distance between the two inclusions in the matrix leads to smaller magnitude of the tangential shear stresses in the matrix on the interface 2. The shear stresses σ_{zs} on the interface in the matrix with higher material ratio $\rho^{(1)} = 2$ are larger than those on the interface in the matrix with lower material ratio $\rho^{(2)} = 0.5$.

7 Conclusions

A closed-form solution is obtained for the mechanical and electric fields of an infinite piezoelectric quasicrystal medium with two circular cylindrical inclusions under antiplane shear and inplane electric loading. Conformal mapping technique and the theorem of analytic continuation are used to solve the boundary value problem. Explicit expressions of the stresses and electric fields in both the matrix and inclusions have successfully been derived. The validity and versatility of the generalized solution in this work have been demonstrated by application to some particular examples, and the influence of the geometric parameters and material properties on the interface stresses was discussed. It is shown that the material properties and the geometric parameters of the composite system and the loading conditions have an effect on the stress distribution.

Acknowledgements The authors wish to thank the Natural Sciences and Engineering Research Council of Canada (NSERC) for its kind support of this research under Discovery Grant (RGPIN-2018-03804). The support from the National Key R&D Program of China (2017YFC0805100) is acknowledged.

References

1. Shechtman, D., Blech, I., Gratias, D., Cahn, J.W.: Metallic phase with long-range orientational order and no translational symmetry. Phys. Rev. Lett. **53**(20), 1951–1953 (1984)
2. Janot, C.: Quasicrystals: a primer. Clarendon Press, Oxford University Press (1993)
3. Louzguine-Luzgin, D.V., Inoue, A.: Formation and properties of quasicrystals. Ann. Rev. Mater. Rev. **38**, 403–423 (2008)
4. Chen, W.Q., Ma, Y.L., Ding, H.J.: On three-dimensional elastic problems of one-dimensional hexagonal quasicrystal bodies. Mech. Res. Commun. **31**, 633–641 (2004)
5. Fan, T.Y., Li, X.-F., Sun, Y.F.: A moving screw dislocation in a one-dimensional hexagonal quasicrystal. Acta Phys. Sinica **8**, 288–295 (1999)
6. Shi, W.C.: Collinear periodic cracks and/or rigid line inclusions of antiplane sliding mode in one-dimensional hexagonal quasicrystal. Appl. Math. Comput. **215**, 1062–1067 (2009)
7. Gao, Y., Ricoeur, A., Zhang, L.L.: Plane problems of cubic quasicrystal media with an elliptic hole or a crack. Phys. Lett. A **375**, 2775–1781 (2011)
8. Sladek, J., Sladek, V., Atluri, S.N.: Path-independent integral in fracture mechanics of quasicrystals. Eng. Fract. Mech. **140**, 61–71 (2015)
9. Loboda, V., Komarov, O., Bilyi, D., Yuri, L.: An analytical approach to the analysis of an electrically permeable interface crack in a 1D piezoelectric quasicrystal. Acta Mech. **231**, 3419–3433 (2020)
10. Li, L.H., Cui, X.W., Guo, J.H.: Interaction between a screw dislocation and an elliptical hole with two asymmetric cracks in a one-dimensional hexagonal quasicrystal with piezoelectric effect. Appl. Math. Mech. **41**, 899–908 (2020)
11. Rao, K.R.M., Rao, P.H., Chaitanya, B.S.K.: Piezoelectricity in quasicrystals: a group-theoretical study. Pramana **68**, 481–487 (2007)
12. Li, X.Y., Li, P.D., Wu, T.H.: Three-dimensional fundamental solutions for one-dimensional hexagonal quasicrystal with piezoelectric effect. Phys. Lett. A **378**, 826–834 (2014)
13. Li, Y., Li, Y., Qin, Q.H., Yang, L.Z., Zhang, L.L., Gao, Y.: Axisymmetric bending analysis of functionally graded one-dimensional hexagonal piezoelectric quasi-crystal circular plate. Proc. R. Soc. A **476**, 20200302 (2020)
14. Yang, J., Li, X.: The anti-plane shear problem of two symmetric cracks originating from an elliptical hole in 1D hexagonal piezoelectric QCs. Adv. Mater. Res. **936**, 127–135 (2014)

15. Yu, J., Guo, J.H., Pan, E., Xing, Y.M.: General solutions of plane problem in one-dimensional quasicrystal piezoelectric material and its application on fracture mechanics. Appl. Mathe. Mech. **82**, 17–24 (2015)
16. Fan, C.Y., Li, Y., Xu, G.T., Zhao, M.H.: Fundamental solutions and analysis of three-dimensional cracks in one-dimensional hexagonal piezoelectric quasicrystals. Mech. Res. Commun. **74**, 39–44 (2016)
17. Tupholme, G.E.: A non-uniformly loaded antiplane crack embedded in a half-space of a one-dimensional piezoelectric quasicrystal. Meccanica **53**, 973–983 (2018)
18. Li, Y.-D., Bao, R.H., Chen, W.Q.: Axial shear fracture of a transversely isotropic piezoelectric quasicrystal cylinder: which field (phonon or phason) has more contribution? Europ. J. Mech./A Solids **71**, 179–186 (2018)
19. Zhou, Y.-B., Li, X.-F.: A Yoffe-type moving crack in one-dimensional hexagonal piezoelectric quasicrystals. Appl. Math. Model. **65**, 148–163 (2019)
20. Hu, K.Q., Jin, H., Yang, Z.J., Chen, X.: Interface crack between dissimilar one-dimensional hexagonal quasicrystals with piezoelectric effect. Acta Mech. **230**, 2455–2474 (2019)
21. Zhao, M.H., Dang, H.Y., Fan, C.Y., Chen, Z.T.: Analysis of a three-dimensional arbitrary shaped interface crack in a one-dimensional hexagonal thermo-electro-elastic quasicrystal bi-material part 1: theoretical solution. Eng. Fract. Mech. **179**, 59–78 (2017)
22. Dang, H.Y., Zhao, M.H., Fan, C.Y., Chen, Z.T.: Analysis of a three-dimensional arbitrary shaped interface crack in a one-dimensional hexagonal thermo-electro-elastic quasicrystal bi-material part 2: numerical method. Eng. Fract. Mech. **180**, 268–281 (2017)
23. Honein, E., Honein, T., Herrmann, G.: On two circular inclusions in harmonic problems. Quart. Appl. Mathe. L **3**, 479–499 (1992)
24. Wu, L.Z.: Interaction of two circular cylindrical inhomogeneities under anti-plane shear. Compo. Sci. Tech. **60**, 2609–2615 (2000)
25. Zou, Z., Li, S.: Stresses in an infinite medium with two similar circular cylindrical inclusions. Acta Mech. **156**, 93–108 (2002)
26. Ma, H.M., Gao, X.-L.: Eshelby's tensors for plane strain and cylindrical inclusions based on a simplified strain gradient elasticity theory. Acta Mech. **211**, 115–129 (2010)
27. Deeg, W.F.: The analysis of dislocation, crack and inclusion problems in piezoelectric solids. Ph. D thesis, Stanford University, Stanford, CA (1980)
28. Meguid, S.A., Zhong, Z.: On the elliptical inhomogeneity problem in piezoelectric materials under antiplane shear and inplane electric field. Int. J. Eng. Sci. **36**, 329–344 (1998)
29. Wu, L.Z., Kunio, F.: The electro-elastic field of the infinite piezoelectric medium with two piezoelectric circular cylindrical inclusions. Acta Mech. Sinica **18**, 368–385 (2002)
30. Yang, B.-H., Gao, C.-F., Noda, N.: Interactions between N circular cylindrical inclusions in a piezoelectric matrix. Acta Mech. **197**, 31–42 (2008)
31. He, L.H., Lim, C.W.: Electromechanical response of piezoelectric fiber composites with sliding interface under anti-plane deformations. Compos. Part B **34**, 373–381 (2003)
32. Wang, X., Pan, E., Roy, A.K.: Interaction between a screw dislocation and a piezoelectric circular inclusion with viscous interface. J. Mech. Mater. Struct. **3**, 761–773 (2008)
33. Zhang, Z.G., Ding, S.H., Li, X.: A spheroidal inclusion within a 1D hexagonal piezoelectric quasicrystal. Arch. Appl. Mech. **90**, 1039–1058 (2020)
34. Muskhelishvili, N.I.: Some basic problems of the mathematical theory of elasticity. Noordhoff, Groningen (1963)
35. Steif, P.S.: Shear stress concentration between holes. ASME J. Appl. Mech. **56**, 719–721 (1989)
36. Zhang, X., Hasebe, N.: Antiplane shear problems of perfect and partially damaged matrix-inclusion systems. Arch. Appl. Mech. **63**, 195–209 (1993)